Title

Modeling Subcellular Protein Recruitment Dynamics for Synthetic Biology

Authors

Badu-Nkansah, Kwabena A

Sernas, Diana

Natwick, Dean E

et al.

Publication Date

2023

DOI

10.1007/978-1-0716-2617-7_10

Modeling Subcellular Protein Recruitment Dynamics for Synthetic Biology

Kwabena A. Badu-Nkansah, Diana Sernas, Dean E. Natwick, and Sean R. Collins*

[1]Department of Microbiology and Molecular Genetics, University of California, Davis, Davis, CA 95616, United States

Running Head/Title: Modelling Protein Recruitment Dynamics

* **Correspondence should be addressed to:**

Sean R. Collins, PhD

Department of Microbiology and Molecular Genetics

University of California, Davis

One Shields Avenue

Davis, CA 95616

E-mail: srcollins@ucdavis.edu

Abstract

Compartmentalized protein recruitment is a fundamental feature of signal transduction. Accordingly, the cell cortex is a primary site of signaling supported by the recruitment of signal regulators to the plasma membrane. Recent emergence of optogenetic strategies designed to control localized protein recruitment has offered valuable toolsets for investigating spatiotemporal dynamics of associated signaling mechanisms. However, determining proper recruitment parameters is important for optimizing synthetic control. In this chapter, we describe a stepwise process for building linear differential equation models that characterize the kinetics and spatial distribution of optogenetic protein recruitment to the plasma membrane. Specifically, we outline how to construct 1) ordinary differential equations that capture the kinetics, efficiency, and magnitude of recruitment and 2) partial differential equations that model spatial recruitment dynamics and diffusion. Additionally, we explore how these models can be used to evaluate the overall system performance and how component parameters can be tuned to optimize synthetic recruitment.

Key Words

Mathematical Modeling, Signal Transduction, Protein Dynamics, Diffusion, Optogenetics, Plasma Membrane, Localization, Compartmentalization, Protein Recruitment, iLID

---

1 Introduction

The cellular cortex is a primary site of signaling where dynamic protein and lipid scaffolds guide signaling networks to control essential cellular behaviors ***(1)***. Signal processing at the plasma membrane occurs through multiple classes of mechanisms including: local

modification of cortical proteins, creation of lipid subdomains that directly recruit protein effectors, and activation of scaffold proteins that promote signal complex formation. In many cases, these processes can be hijacked by controlling the localization of specific pathway components. As a result, a number of engineered strategies that mimic primary modes of protein recruitment to the plasma membrane have emerged as complementary toolsets in synthetic biology for investigating compartmentalized dynamics of signal transduction (Figure 1).

Engineered control of protein localization typically uses chemical***(2–5)*** and/or light-inducible***(6–8)*** strategies. In general, these tools rely on tagging a target signal regulator and its binding partner(s) separately with genetically encoded affinity domains whose associations require exogenous activation. These approaches can also be adapted to locally recruit constitutively active regulators to cellular compartments of interest that house important effectors ***(6)***. Accordingly, exogenous recruitment of target proteins to the cell cortex can be achieved by anchoring one dimerization component to the inner leaflet of the plasma membrane. This strategy has been employed to selectively activate and recruit Rho GTPases ***(9, 10)***, control spindle positioning ***(11)***, investigate lipid regulation of ion channels ***(12)***, and decipher actin mediated Phosphoinositide 3-kinase feedback during cell polarization ***(13, 14)***. In addition to activating downstream signaling, synthetic recruitment strategies have also been used for inhibitory roles by sequestering protein regulators away from their signaling niches ***(15)***. The increasing diversity of synthetic strategies for protein recruitment and control have immense potential for elucidating complex signaling networks. However, these systems are built from biochemical components bound by the laws of chemistry and physics. Often their behaviors in real cells do not match the cartoon models that we draw based on their design, and system responses can be variable from cell to cell and from day to day. Computational methods provide a natural complement for these approaches by assessing how component features can be tuned to elicit desired dynamics. When component parameters are known, or can be empirically estimated, mathematical models can become powerful tools that offer predictability

and insights into how biochemical and physical constraints affect system performance. They can be particularly useful for characterizing the kinetics and spatial patterns of component outputs after compartmentalized recruitment.

Here, we describe a stepwise approach to construct and apply mathematical models to characterize the kinetics and spatial distribution of protein recruitment ***(7)***. We describe the construction of a system of ordinary differential equations (ODEs) to analyze the temporal dynamics of protein recruitment and partial differential equations (PDEs) that incorporate spatial patterns. Such ODE/PDE models have been useful in profiling membrane associated processes including EGF receptor mediated MAPK signaling ***(16)***, optogenetic membrane anchoring ***(7)***, signal transmission from compartmentalized Ras GTPase nanoclusters ***(17)***, and membrane associated Rho GTPase cycling ***(18–20)***. To illustrate this approach, we specifically focus on a two-component ODE model that encompasses the dynamics of local recruitment of a protein species to the plasma membrane. We also derive an associated PDE model that incorporates spatial conditions, symmetry features, and the effect of diffusion on conferring spatial association patterns. We describe how to compute these models using MATLAB; however, similar computational strategies can be implemented using other programming languages.

---

2 Materials

Personal Computer;

A programming platform such as MATLAB equipped with algorithmic solvers for systems of ODEs and/or 1-D PDEs

---

3 Methods

3.1: Modeling Recruitment Kinetics and Endpoint Dynamics

A key challenge in designing synthetic recruitment systems is achieving high levels of stimulus-induced responses with low basal recruitment. In general, the rate of membrane recruitment and the rate of dissociation are critical parameters that need to be optimized for this goal. We recently generated models to explore these features for a popular optogenetic approach, the Improved Light Induced Dimerization (iLID) system ***(7)***. iLID is an engineered protein containing a modified LOV2 domain that, in response to light, exposes a peptide from *E. coli* SsrA capable of binding with high affinity to a partner SspB fusion protein (Figure 2A) ***(6)***. By anchoring iLID to the plasma membrane, this system can be used to concentrate target proteins of interest to local membrane sites in response to blue light exposure. In addition to intrinsic features that control component binding, including component conformation dynamics and binding specifications of the SsrA peptide and SspB, recruitment performance of iLID depends on extrinsic variables, such as component concentrations and compartmental anchoring, that often require empirical optimization by the user. However, in silico approaches can be useful for identifying parameters that help guide recruitment optimization.

To predict the behavior of such a system, we can construct ODE models to identify expression regimes of component species for which membrane recruitment is specific and efficient. Our simple model contains two protein species where a substrate (S) concentrates to the plasma membrane upon activation of the recruiting receptor species (R) (Figure 2B). We consider the [iLID] and [SspB] components as representations of [R] and [S], respectively, but a structurally identical model can also be used to describe other optogenetic approaches or, alternatively, simple systems of localized protein recruitment. In this model, R is bistable, it can exist either in an inactive state with low affinity for substrate S or as a high affinity active state,

R* (Figure 2B). It is critical to consider binding for both states of R, as the basal binding of S to inactive R can be a key limitation of recruitment systems at high component concentrations.

Here we describe how to outline the primary states of the system and build an ODE model that captures the kinetics of protein recruitment. After defining component species, interaction states, and reaction events, initial conditions prior to receptor activation can be determined.

1. Define the molecular components of the system, systematically determine each state of the system and each possible transition between states. For our model, this corresponds to the diagram in Figure 2B.

2. Assign variables to the protein species and component states involved in recruitment. Be sure to have a variable for every molecular species in the model:

Protein Species

R = Free Inactive Receptor

R = Free Active Receptor*

S = Free Substrate

RS = Bound Inactive Receptor-Substrate

*R*S = Bound Active Receptor -Substrate*

3. Write chemical equations for each reaction in the model, including component interactions and transitions between protein states. We assume that receptor activation occurs in response to the experimental stimulation with a single rate that is equal for all binding states of the receptor. For this example, receptor activation rate, γ, will be nonzero during stimulation and zero otherwise:

Interaction Events

$R + S \rightleftharpoons RS$; *Forward Rate* = $Rate_{Inactive,Binding}$; *Reverse Rate* = $Rate_{Inactive,Release}$

$R^* + S \rightleftharpoons R^*S$; *Forward Rate* = $Rate_{Active,Binding}$; *Reverse Rate* = $Rate_{Active,Release}$

Receptor Activation Events

$R \rightleftharpoons R^*$; *Forward Rate* = γ; *Reverse Rate* = $Rate_{Rev}$

$RS \rightleftharpoons R^*S$; *Forward Rate* = γ; *Reverse Rate* = $Rate_{Rev}$

4. Define reaction constants. We can define the rate constant numerically using estimates based on published measurements. In many cases, the binding affinities (K_d) may be available, but the forward and reverse binding rates may not be. In this case, we relate both rates to the K_d, and estimate the off-rate using published kinetic data or by calibrating the model to empirical measurements (Note 1).

$$K_{d,inactive} = \frac{Rate_{Inactive,Release}}{Rate_{Inactive,Binding}}$$

We will treat the forward rate of receptor activation (γ) as an experimental input into the model, but the associated reverse rate can likely be empirically obtained or estimated from observations made in prior literature.

5. Define mathematical versions of the rate equations for each species. Construct one differential equation for each species in the model (Note 2). To simulate receptor activation, the receptor activation term, γ_{input}, will depend on the external input at a given time. For iLID systems γ_{input} is the temporal profile of blue light irradiation:

(1) $$\frac{d[R^*]}{dt} = \gamma_{input} * [R] + Rate_{Active,Release} * [R^*S] - Rate_{Active,Binding} * [R^*] * [S] - Rate_{Rev} * [R^*]$$

(2) $$\frac{d[R^*S]}{dt} = \gamma_{input} * [RS] + Rate_{Active,Binding} * [R^*] * [S] - Rate_{Active,Release} * [R^*S] - Rate_{Rev} * [R^*S]$$

(3) $$\frac{d[R]}{dt} = Rate_{Inactive,Release} * [RS] + Rate_{Rev} * [R^*] - Rate_{Inactive,Binding} * [R] * [S] - \gamma_{input} * [R]$$

$$(4)\ \frac{d[RS]}{dt} = Rate_{Inactive,Binding} * [R] * [S] + Rate_{Rev} * [R^*S] - Rate_{Inactive,Release} * [RS] - \gamma_{input} * [RS]$$

$$(5)\ \frac{d[S]}{dt} = Rate_{Inactive,Release} * [RS] + Rate_{Active,Release} * [R^*S] - Rate_{Inactive,Binding} * [R] * [S] - Rate_{Active,Binding} * [R^*] * [S]$$

6. Define the initial state of the system. Prior to stimulation, we assume that the receptor is entirely inactive, and the system is in steady state. Therefore, each reaction species can be defined using known measurements. At this initial state, variables $[R]_{total}$ and $[S]_{total}$ are defined to be constants representing the total concentration of the two proteins. Additionally, conservation of mass can be used to relate free [R] and [S] to the amount of complexed [RS]:

$$[R^*] = 0;$$
$$[R^*S] = 0;$$
$$[R] = [R]_{total} - [RS];$$
$$[S] = [S]_{total} - [RS];$$

$$(6)\ \frac{d[RS]}{dt} = Rate_{Inactive,Binding} * [R] * [S] - Rate_{Inactive,Release} * [RS]$$

7. Compute the concentration of RS at steady state by setting the rate d[RS]/dt (Eq. 6) to zero:

$$(7)\ 0 = Rate_{Inactive,Binding} * [R] * [S] - Rate_{Inactive,Release} * [RS] \quad (At\ steady\ state)$$

$$(8)\ 0 = ([R]_{total} - [RS]) * ([S]_{total} - [RS]) - K_d * [RS]$$

$$(9)\ 0 = [RS]^2 + [R]_{total} * [S]_{total} - [RS] * [R]_{total} - [RS] * [S]_{total} - K_d * [RS]$$

$$(10)\ 0 = [RS]^2 - ([R]_{total} + [S]_{total} + K_d) * [RS] + ([R]_{total} * [S]_{total})$$

$$(11)\ [RS] = \frac{([R]_{total} + [S]_{total} + K_d) \pm \sqrt{([R]_{total} + [S]_{total} + K_d)^2 - 4 * ([R]_{total} * [S]_{total})}}{2}$$

$$(11') \; [RS] = \frac{b - \sqrt{b^2 - 4 * ([R]_{total} * [S]_{total})}}{2} \; ; \; b = \; [R]_{total} \; + [S]_{total} + \; K_d$$

8. Now that rate equations for each reaction species and initial conditions are defined, reaction kinetics can be computed and the ODEs solved algorithmically. We have customarily used the MATLAB ODE solver function, *ode45,* for this; however, similar algorithmic solvers of ODEs can be found in many other programming languages (Note 3).

3.2: Analyzing Efficiency of Recruitment

This approach can be customized to simulate kinetic dynamics of a variety of synthetic recruitment strategies by using different choices of component concentrations, dissociation constants, and activation/inactivation rates of the receptor (Note 4). Here we will briefly display example model performance measures using values determined for iLID-mediated recruitment. As a general note, we suggest simulating the model for a few choices of concentrations first to verify that the output looks reasonable and to gain an intuition for the model.

1. The computed system of ODEs can be evaluated by analyzing notable features of model outputs. For example, basal recruitment, maximum recruitment, fold recruitment, and dissociation each designate performance measures that help guide optimization strategies for efficient synthetic recruitment (Figure 3). Basal recruitment can be computed from the initial steady state of the model, while the other measures can be determined from the simulated model output (Figure 4A). Max absolute recruitment can be determined from the steady state solution during extended system input, similar to how initial conditions were calculated in the previous section (Figure 4D). Fold recruitment can be calculated using computed values for basal and max recruitment (Figure 4G). Kinetic parameters such as $t_{1/2}$ of dissociation are computed from temporal profiles for simulations involving transient

system input (Figure 4J). After analyzing the model across systematic ranges of concentrations for each component, heatmap plots can be used to visualize how each performance measure depends on component concentrations (Figure 4B, 4E, 4H, 4K). Each pixel in the heatmap represents outputs from model simulations using specific combinations of parameters (Figure 4C, 4F, 4I, 4L; *Top*) (Note 5). Lastly, analogous plots can also be generated to visualize how performance depends on additional variables such as rate constants and component binding affinity characteristics.

2. Model output interpretation: Ideally, performance measures generated from model simulations can generally predict how recruitment parameters and component characteristics influence recruitment efficiency. For example, our system of ODEs generally predicts that both basal and maximum membrane recruitment scale positively with increasing component concentrations (Figure 4C, 4F; *Bottom*). While this trade-off limits system performance, the simulation results can be used to understand how fold recruitment scales with component concentrations (Figure 4I; *Bottom*) and identify ranges of component concentrations where system performance is most efficient. By defining threshold values for parameters of interest, an ideal concentration space can be determined where system performance exceeds each threshold. These results can be used to guide experimental design and troubleshoot parameters where synthetic recruitment is not performing as desired. Furthermore, the model can make less intuitive predictions. For example, our iLID ODE model predicted that global iLID-SspB disassociation rates decrease with increasing iLID concentration***(7)*** (Figure 4L; *Bottom*). This effect arises from newly dissociated SspB molecules being more likely to re-bind at the membrane if surrounding levels of unbound iLID are high.

3.3: Modeling Spatial Dynamics of Recruitment

Models generated from ODEs typically capture dynamics across a single dimension and are therefore suitable for determining the temporal evolution of reaction systems. However, in addition to kinetic features, cell signaling mechanisms often rely on spatially heterogeneous patterns. For protein interactions at the plasma membrane, cytoplasmic diffusion near the cell cortex and lateral diffusion along the membrane are important factors that influence spatial distributions of recruitment events. Additionally, functional outputs of biological signaling are often determined by spatially asymmetric propagation of signaling circuitry. Partial differential equations (PDEs) follow system dynamics across multiple independent variables and are useful for capturing how system components change in space and time. Here we will generate a PDE model that illustrates how diffusion affects the spatial distribution of recruitment over time. Towards this goal, consider the general diffusion equation for temporal change in concentration of a chemical species over a 1-dimensional spatial coordinate:

$$(12)\ \frac{\partial u}{\partial t} = D\,\frac{\partial^2 u}{\partial x^2}$$

where $u(x,t)$ represents a concentration value of species u at position x and time t. Additionally, $\frac{\partial u}{\partial t}$ represents the change of concentration of *u* over time, $\frac{\partial^2 u}{\partial x^2}$ describes the profile of concentration across the spatial coordinate x, and D is the diffusion coefficient within the system.

We can build our PDE model based on our previous ODE model through the following steps:

1. Determine the spatial domain for the model. Using a 1-dimensional domain simplifies computation and the interpretation of model results. We can modify symmetry to model higher dimensional geometries using this simple domain. For analyzing the spatial spread of proteins on a 2-dimensional plasma membrane, we define our spatial coordinate to be the

radial distance along the membrane from the target recruitment site. We use symmetry conditions in the model, to handle the increasing area associated with larger radial distances. This is accomplished in MATLAB's *pdepe* PDE solver by setting the symmetry parameter *m* to 1 for "cylindrical" symmetry (Note 6).

2. Define the diffusion coefficients. The diffusion coefficients are the only additional parameters for this model (Note 7).

3. Define the molecular species within the variable *u*. Importantly, $u(x,t)$ can represent a single concentration species across the spatial coordinate x and time coordinate t; or, for signaling circuits that involve multiple reaction species, a matrix that incorporates all relevant species within the system:

$$(13)\ u(x,t) = \begin{bmatrix} u_1 \\ u_2 \\ u_3 \\ u_4 \\ u_5 \end{bmatrix};$$

where $u_1 = [R]$, $u_2 = [R^*]$, $u_3 = [RS]$, $u_4 = [R^*S]$, $u_5 = [S]$.

For our purposes, we interpret the units for the spatial dimension to be in microns since this is a relevant scale for a cell.

4. To build a PDE, spatial boundary conditions must also be defined. We typically use the Neumann condition (Note 8), specifying that the spatial derivative is zero at the boundaries:

$$\frac{du}{dx} = 0;\ at\ x = 0\ and\ x = x_{max}$$

5. In contrast to the ODE example, we will now assume that this system begins with a pre-established profile of active receptors. This approach is useful for analyzing the spread of

recruited components after an initial standardized input. Therefore, initial conditions can be adapted as follows:

$$u_1 = 0;$$

$$u_2 = ([R]_{total} - [R^*S]) \ * \ r(x)\,;$$

$$u_3 = 0;$$

$$u_4 = \left(\frac{b - \sqrt{b^2 - 4 * ([R]_{total} * [S]_{total})}}{2}\right) * \ r(x), \ \ where\ b = \ [R]_{total} \ + [S]_{total} + \ K_d;$$

$$u_5 = [S]_{total} - [R * S]$$

where $r(x)$ is a scaling function that determines the spatial distribution of receptor activation. For example, in optogenetic systems such as iLID, after global light activation, $r(x)$ can be set to a gaussian profile peaking at x=0, with a width determined by the resolution of focal stimulation for an optical microscope system.

6. For algorithmic evaluation of PDE models, programmatic solvers often require representing PDEs in standard organizational forms. In MATLAB a standard form for 1D PDE solvers is:

$$(14)\ c\left(x, t, u, \frac{\partial u}{\partial x}\right)\frac{\partial u}{\partial t} \ = \ x^{-m}\frac{\partial}{\partial x}\left(x^m\, f\left(x, t, u, \frac{\partial u}{\partial x}\right)\right) + s\left(x, t, u, \frac{\partial u}{\partial x}\right)$$

where $f\left(x, t, u, \frac{\partial u}{\partial x}\right)$ is a term for the temporal and spatial flux of the species *u*, $s\left(x, t, u, \frac{\partial u}{\partial x}\right)$ is a source term or reaction term that, in this case, will incorporate binding and chemical reactions that generate or deplete species within *u*, and $c\left(x, t, u, \frac{\partial u}{\partial x}\right)$ represents a balance coefficient. *m* is the symmetry constant that determines the type of spatial symmetry in the system; m = 0, 1, or 2 represents cartesian (no symmetry), cylindrical symmetry (azimuthal), or spherical symmetry (azimuthal and zenith) coordinates respectively.

7. Referring to the initial equation for diffusion (eq. 12), with an addition of the reaction term, its standard form can be rewritten as:

$$(15)\ \frac{\partial u}{\partial t} = \frac{\partial}{\partial x}\left(D\ \frac{\partial u}{\partial x}\right) + s\left(u(x,t), \frac{\partial u}{\partial x}\right)$$

where:

$$c\left(x,t,u,\frac{\partial u}{\partial x}\right) = 1;$$

$$f\left(x,t,u,\frac{\partial u}{\partial x}\right) = D\ \frac{\partial u}{\partial x}$$

In this system, the source term *s* corresponds to the same set of terms as the right-hand side of the equations from our ODEs generated previously (eq. 1-5). Collectively, these equations can be written in matrix form as $s\left(u(x,t), \frac{\partial u}{\partial x}\right)$ (Note 9):

$$\begin{bmatrix} S_1 \\ S_2 \\ S_3 \\ S_4 \\ S_5 \end{bmatrix} = \begin{bmatrix} Rate_{Inactive,Release} * u_3 + Rate_{Rev} * u_2 - Rate_{Inactive,Binding} * u_1 * u_5 \\ Rate_{Active,Release} * u_4 - Rate_{Active,Binding} * u_2 * u_5 - Rate_{Rev} * u_2 \\ Rate_{Inactive,Binding} * u_1 * u_5 + Rate_{Rev} * u_4 - Rate_{Inactive,Release} * u_3 \\ Rate_{Active,Binding} * u_2 * u_5 - Rate_{Active,Release} * u_4 - Rate_{Rev} * u_4 \\ Rate_{Inactive,Release} * u_3 + Rate_{Active,Release} * u_4 - Rate_{Inactive,Binding} * u_1 * u_5 - Rate_{Active,Binding} * u_2 * u_5 \end{bmatrix}$$

8. At this stage, with the initial and boundary conditions set, the PDEs can be integrated using programmatic solvers such as *pdepe* function in MATLAB (Note 10).

3.4: Analyzing Recruitment and Diffusional Spread

1. Just as with the ODE model, measures of system performance should be computed. While basal recruitment can be computed similarly, maximal recruitment will be different since PDE models simulate recruitment in a local subregion of the plasma membrane that evolves over time (Figure 5A). In this case, both dissociation and diffusional spread can reduce the

local accumulation of the recruited protein. For this reason, maximal recruitment should be determined by following simulation outputs over time. Additionally, the dependence of recruitment on the concentrations of R and S will likely scale differently from what was previously produced in the ODE model.

2. Compared to ODE simulations, the PDE model naturally presents additional measures of system performance. Most notably, the spread of recruitment regions can be calculated from the spatial recruitment profiles at given component concentrations and diffusion characteristics (Figure 5A).

3. As with the ODE model, thresholds for the PDE system can be set for each measure of system performance. Regions in component concentration spaces that exhibit acceptable recruitment performances can be identified and subsequently used to inform how synthetic systems can be optimized at the bench (Figure 5B, 5D, 5F). For example, we have used similarly structured PDE models to optimize iLID recruitment approaches. These PDE models profiled how customizing plasma membrane anchoring strategies that confer differential membrane diffusion properties to iLID receptors influence spatiotemporal SspB recruitment (Note 11,12). PDE modeling of iLID recruitment offered interesting predictions. Constraining receptor diffusion at the membrane by increasing membrane anchor size resulted in significant changes in substrate recruitment levels. This model predicted that decreasing receptor diffusion promoted increased maximum recruitment, fold recruitment, and lengthened evolution time to maximal recruitment of substrate across wide ranges of receptor and substrate concentrations (Figure 5C, 5E, 5G).

Altogether, two-component ODE and PDE models reliably captures fundamental features of protein recruitment dynamics. With proper reaction constants and measures for component

features in hand, modeling approaches like these can be implemented in a straightforward manner. Additionally, these analytical approaches offer powerful predictive strength for synthetic recruitment strategies and can provide unique insights into efficient manipulation of compartmentalized signaling using synthetic tools.

---

4 Notes

1. To estimate the kinetic binding and dissociation rates, one can make some simplifying assumptions. In many cases, binding affinities are determined largely by the dissociation rates. For simplicity, we can assume that the association rates are equal for inactive and active forms of R. We then can estimate or calibrate the association and dissociation rates from kinetic experiments measuring the half-time for association after a strong light stimulus. Importantly, association rates are likely to be different for different optogenetic systems. For example, the “magnets” system was designed to have a more rapid association rate ***(21, 22)***.

2. It is essential that as differential equations are built, balance is maintained according to the law of conservation of mass. This can be checked by making sure that, for each equation, all events that either produce or consume the target component species are represented.

3. In many cases, γ_{input} will be a step function. These are typically not handled well by numerical integration algorithms such as *ode45*. A handy solution to this problem is to perform piecewise numerical integration. One can separately perform numerical integration for each time period in which γ_{input} is constant, using the output of each round of numerical integration as the initial condition for the next. For example, a simple experiment where γ_{input}

is 1 for the first and second round and then zero thereafter would require two separate rounds of numerical integration with the second using the conditions produced by the first round.

4. Accurate estimations for component concentrations, dissociation constants, and reaction rates can improve predictive ability of ODE/PDE models. For modeling iLID recruitment we use an assortment of values either derived empirically or approximated using measurements from similar mechanisms. The following parameter values have been useful for modeling iLID dynamics (with associated references):

$$Total\ [iLID] = 0.1\mu M$$

$$Total\ [SspB] = 0.5\mu M$$

$$K_{d,Lit(active)} = 130nM \quad \textbf{(6)}$$

$$K_{d,Dark(inactive)} = 4.7\mu M \quad \textbf{(6)}$$

$$Rate_{iLID\ Reversal} = 0.02\ s^{-1} \quad \textbf{(21)}$$

$$Rate_{disassociation,Lit} = 0.5\ s^{-1} \quad \textbf{(21)}$$

5. Model outputs may evolve over time, therefore it is important to verify that simulations are run over long enough time periods to determine the correct value.

6. While cylindrical symmetry is useful for simulating spot recruitment and diffusion along a flat membrane interface, in other cases it may be useful to model diffusion of a cytoplasmic component towards or away from the membrane in a spherical cell. For the latter, the symmetry parameter *m*, in MATLAB's *pdepe* PDE solver, can be set to 2 for designating spherical (azimuthal and zenith) symmetry coordinates.

7. Diffusion coefficients can be determined empirically, for instance through fluorescence recovery after photobleaching experiments. As a rough guide, diffusion coefficients may be around 10-30 $\mu m/s^2$ for cytoplasmic proteins, 0.5-1 $\mu m/s^2$ for lipid-anchored proteins, and 0.03-0.1 $\mu m/s^2$ for transmembrane proteins.

8. The Neumann boundary condition specifies that the spatial derivative of a system is constant at its boundaries. By setting the derivative to zero at each boundary, the resulting condition can be thought of as a "reflecting" boundary which maintains the flux of model components within the spatial barriers of the system. Therefore, under this condition, there is no passage of molecular species in or out of the system through the boundary which helps ensure conservation of mass.

9. Note that the source term *s* for the PDEs encompasses kinetic parameters and interaction states of component species. To also incorporate light input, $s\left(x, t, u, \frac{\partial u}{\partial x}\right)$ can include a γ_{input} term that designates a temporal profile of blue light activation such as in equation (1-5).

10. Note that while PDE solvers in other programming languages may have similar requirements for initial conditions, boundary conditions, source, and flux terms, they may require different organizational formats for proper implementation.

11. For this example, we implemented a PDE model of iLID diffusion where membrane diffusion coefficients for iLID-CAAX (short anchor) and Stargazin-iLID (long multipass anchor) were estimated to be 1 $\mu m^2/s$ and 0.1 $\mu m^2/s$, respectively, based on observations from previous studies ***(23, 24)***.

12. Custom MATLAB code for implementing both ODE and PDE models designed for iLID recruitment can be found at: https://github.com/srcollins/Code_for_iLID_Recruitment_from_Springer-Protocol-Chapter-2022

Acknowledgement

We would like to thank the following funding sources for their support of this work. SRC thanks the NIH for the Director's New Innovator Award DP2-HD-094656. DEN thanks the NIH for the F31 Fellowship F31 HL152621, DS thanks the NIH T32 GM099608 training program, while KABN thanks the NIH T32 CA108459 training program for support.

References

1. Grecco HE, Schmick M, and Bastiaens PIH (2011) Signaling from the living plasma membrane. Cell 144:897–909
2. Ho SN, Biggar SR, Spencer DM, et al (1996) Dimeric ligands define a role for transcriptional activation domains in reinitiation. Nature 382:822–6
3. Spencer DM, Wandless TJ, Schreiber SL, et al (1993) Controlling signal transduction with synthetic ligands. Science 262:1019–24
4. Komatsu T, Kukelyansky I, McCaffery JM, et al (2010) Organelle-specific, rapid induction of molecular activities and membrane tethering. Nat Methods 7:206–8
5. Miyamoto T, DeRose R, Suarez A, et al (2012) Rapid and orthogonal logic gating with a gibberellin-induced dimerization system. Nat Chem Biol 8:465–70
6. Guntas G, Hallett RA, Zimmerman SP, et al (2015) Engineering an improved light-

induced dimer (iLID) for controlling the localization and activity of signaling proteins. Proc Natl Acad Sci U S A 112:112–7

7. Natwick DE and Collins SR (2021) Optimized iLID Membrane Anchors for Local Optogenetic Protein Recruitment. ACS Synth Biol 10:1009–1023
8. Zimmerman SP, Hallett RA, Bourke AM, et al (2016) Tuning the Binding Affinities and Reversion Kinetics of a Light Inducible Dimer Allows Control of Transmembrane Protein Localization. Biochemistry 55:5264–71
9. O'Neill PR, Castillo-Badillo JA, Meshik X, et al (2018) Membrane Flow Drives an Adhesion-Independent Amoeboid Cell Migration Mode. Dev Cell 46:9-22.e4
10. O'Neill PR, Kalyanaraman V, and Gautam N (2016) Subcellular optogenetic activation of Cdc42 controls local and distal signaling to drive immune cell migration. Mol Biol Cell 27:1442–50
11. Okumura M, Natsume T, Kanemaki MT, et al (2018) Dynein-Dynactin-NuMA clusters generate cortical spindle-pulling forces as a multi-arm ensemble. Elife 7
12. Suh B-C, Inoue T, Meyer T, et al (2006) Rapid chemically induced changes of PtdIns(4,5)P2 gate KCNQ ion channels. Science 314:1454–7
13. Inoue T and Meyer T (2008) Synthetic activation of endogenous PI3K and Rac identifies an AND-gate switch for cell polarization and migration. PLoS One 3:e3068
14. Graziano BR, Gong D, Anderson KE, et al (2017) A module for Rac temporal signal integration revealed with optogenetics. J Cell Biol 216:2515–2531
15. Robinson MS, Sahlender DA, and Foster SD (2010) Rapid inactivation of proteins by rapamycin-induced rerouting to mitochondria. Dev Cell 18:324–31
16. Huang CY and Ferrell JE (1996) Ultrasensitivity in the mitogen-activated protein kinase cascade. Proc Natl Acad Sci U S A 93:10078–83
17. Tian T, Harding A, Inder K, et al (2007) Plasma membrane nanoswitches generate high-fidelity Ras signal transduction. Nat Cell Biol 9:905–14

18. Goryachev AB and Pokhilko A V (2006) Computational model explains high activity and rapid cycling of Rho GTPases within protein complexes. PLoS Comput Biol 2:e172
19. Jilkine A, Marée AFM, and Edelstein-Keshet L (2007) Mathematical model for spatial segregation of the Rho-family GTPases based on inhibitory crosstalk. Bull Math Biol 69:1943–78
20. Mori Y, Jilkine A, and Edelstein-Keshet L (2008) Wave-pinning and cell polarity from a bistable reaction-diffusion system. Biophys J 94:3684–97
21. Benedetti L, Barentine AES, Messa M, et al (2018) Light-activated protein interaction with high spatial subcellular confinement. Proc Natl Acad Sci U S A 115:E2238–E2245
22. Kawano F, Suzuki H, Furuya A, et al (2015) Engineered pairs of distinct photoswitches for optogenetic control of cellular proteins. Nat Commun 6:6256
23. Yanagawa M, Hiroshima M, Togashi Y, et al (2018) Single-molecule diffusion-based estimation of ligand effects on G protein-coupled receptors. Sci Signal 11
24. Hoze N, Nair D, Hosy E, et al (2012) Heterogeneity of AMPA receptor trafficking and molecular interactions revealed by superresolution analysis of live cell imaging. Proc Natl Acad Sci U S A 109:17052–7

Figure 1: Signaling mechanisms for plasma membrane recruitment with example design principles of associated optogenetic systems.

A) *Left,* Cortical protein recruitment by receptor activation and clustering. *Right,* Synthetic activation driven by CRY2 optogenetic receptor clustering.

B) *Left,* Direct associations between plasma membrane lipid domains and lipid binding proteins. *Right,* Local protein recruitment to plasma membrane domains after synthetic enrichment of signaling lipids using iLID optogenetic recruitment of a lipid modifying enzyme.

C) *Left,* Signaling complex formation downstream of an activated receptor. *Right,* Synthetic production of signaling complexes through direct stimulation of optogenetic opsin receptors.

Figure 2: Schematic diagrams of iLID recruitment and component interaction states.

A) Diagram illustrating idealized iLID and SspB interactions before and after light activation.

B) Schematic diagram depicting possible activation states and interaction events during membrane recruitment of substrate S by receptor R, including “dark state binding” in which the substrate binds to an inactive membrane receptor.

Figure 3: Representative plot of recruitment kinetics after receptor activation.

Depiction of an example kinetic profile of recruitment after temporary receptor stimulation. Illustrated here are measures of recruitment dynamics captured in ODE/PDE models including: basal recruitment, max recruitment, fold enrichment, and $t_{1/2}$ of dissociation.

Figure 4: ODE modeling captures important features of recruitment dynamics across broad ranges of component expression regimes.

A,D,G,J) Example plot profiles of recruitment kinetics each illustrating a measurement feature captured by ODE modeling.

B,E,H,K) Heatmap plots generated from ODE models displaying individual features of recruitment across four orders of magnitude of [R] and [S] concentrations. In these examples, values represent real recruitment measures predicted by ODE models constructed for iLID-SspB interactions. Red bars designate isolated concentration regions portrayed in C,FI, and L.

C,F,I,L) *Top*, Heat map insets of specific regions extracted from B,E,H, and K (red bars) showing differential dynamics between two different receptor concentrations. *Bottom,* Line trace format of heat map insets comparing recruitment features at two different receptor concentrations.

Figure 5: PDE modeling captures the effects of receptor diffusion on spatial spread and recruitment dynamics across broad ranges of component expression levels.

A) Time lapse plots displaying spatial spread of recruitment predicted by PDE modeling. Additionally, important measures of recruitment are depicted including: max recruitment, basal recruitment, time to max recruitment, and recruitment spread.

B,D,F) Heat map plots generated from PDE models displaying the effect of receptor diffusion on individual features of recruitment across ranges of [R] and [S] concentrations. In these examples, values represent real recruitment measures predicted by PDE simulations of iLID-SspB interactions with two different membrane anchors (see Note 10). Red bars designate isolated concentration regions portrayed in C, E, and G.

C,E,G) Line traces of heat map insets (red bars) from B, D, and F comparing the effect of changing receptor diffusion on individual recruitment features across a range of receptor concentrations.

Figure 1

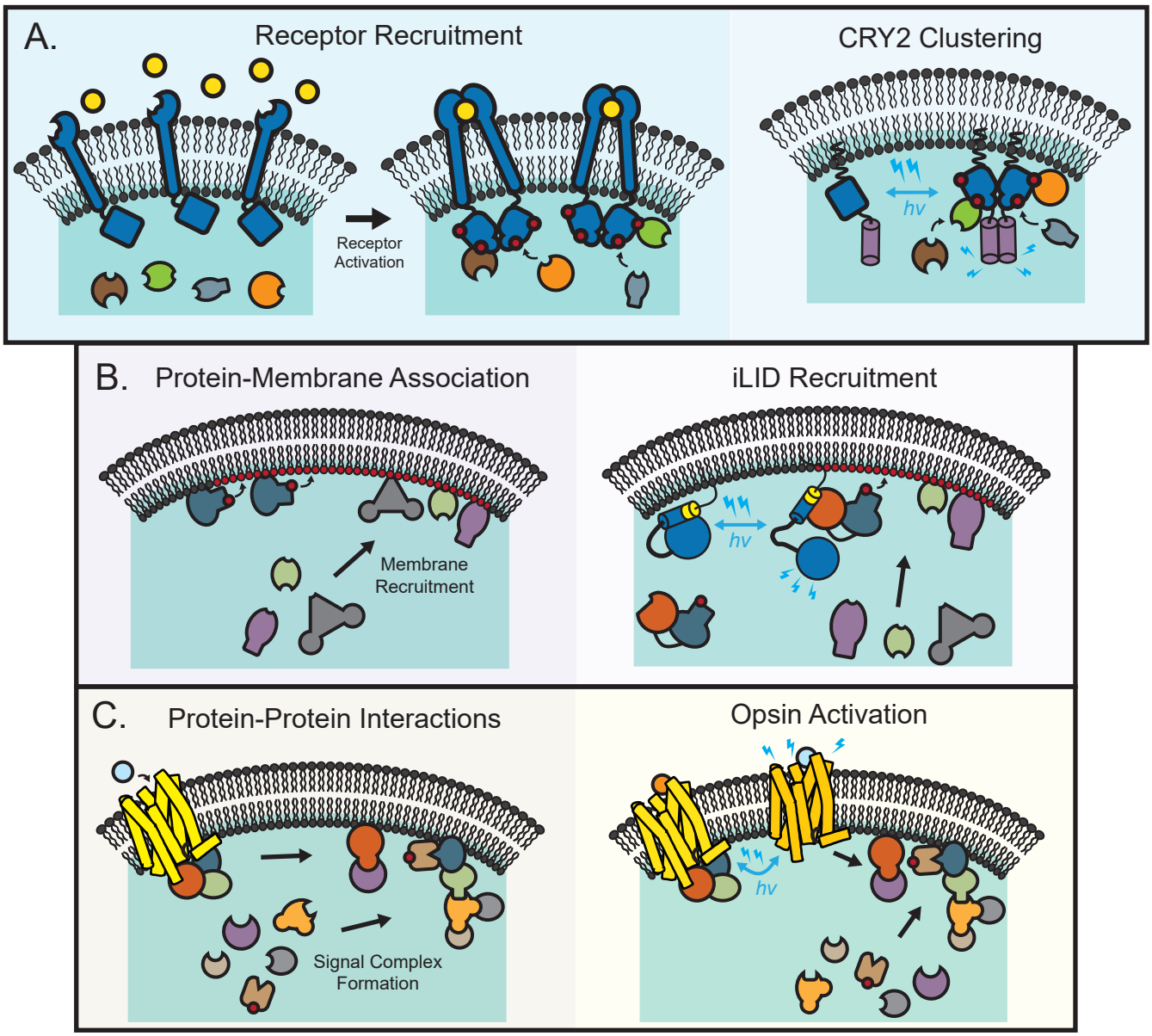
A.
Receptor Recruitment
Receptor
Activation
CRY2 Clustering
hv
B.
Protein-Membrane Association
Membrane
Recruitment
iLID Recruitment
hv
C.
Protein-Protein Interactions
Signal Complex
Formation
Opsin Activation
hv

Figure 2

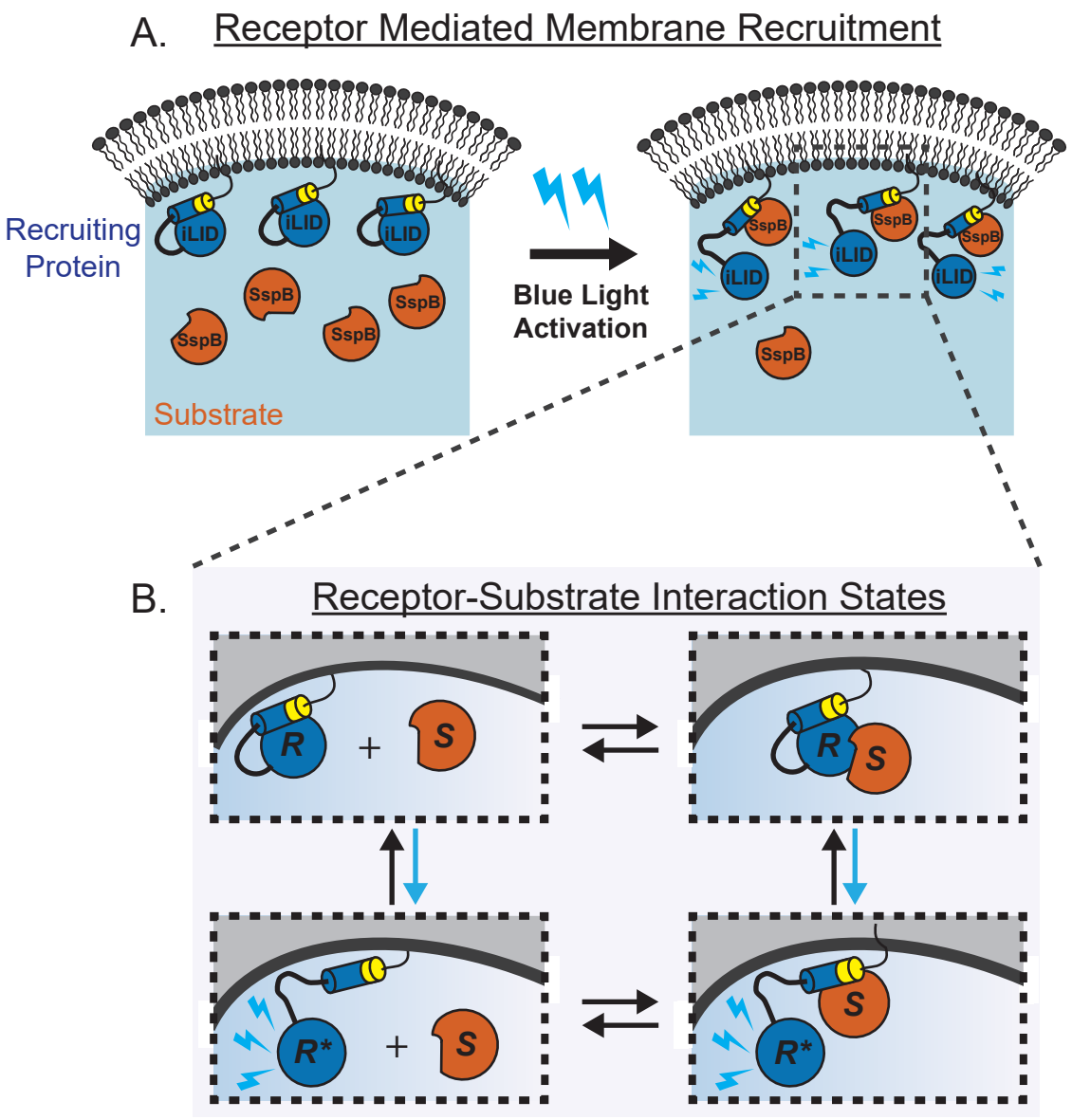
A. Receptor Mediated Membrane Recruitment
Recruiting Protein
iLID
SspB
Substrate
Blue Light Activation
B. Receptor-Substrate Interaction States
R
S
R*

Figure 3

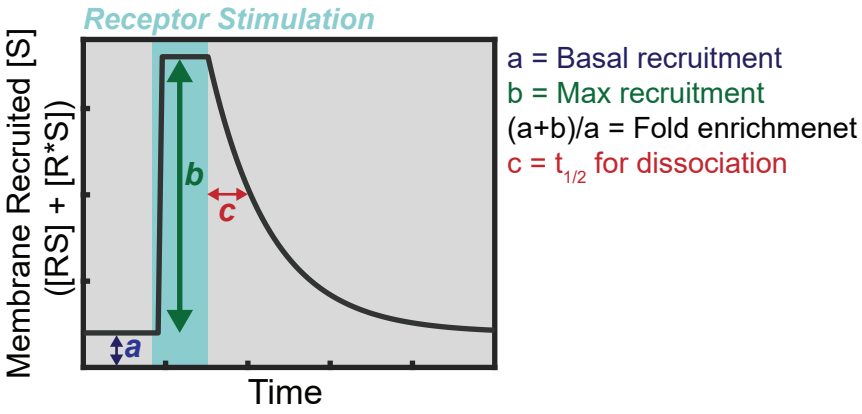
Receptor Stimulation
Membrane Recruited [S]
([RS] + [R*S])
a
b
c
Time
a = Basal recruitment
b = Max recruitment
(a+b)/a = Fold enrichmenet
c = t1/2 for dissociation

Figure 4

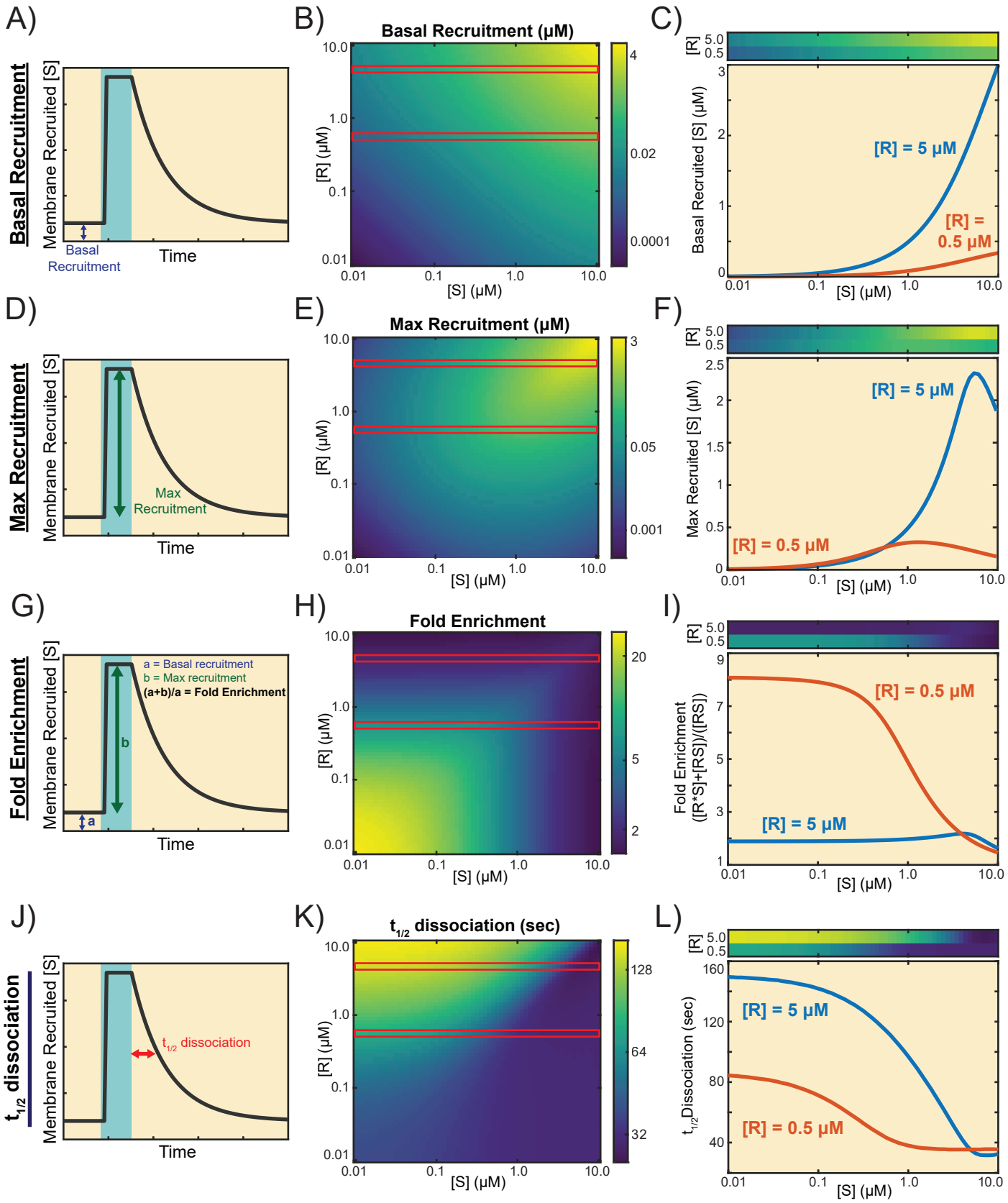
A)
Basal Recruitment
Membrane Recruited [S]
Basal Recruitment
Time
B)
Basal Recruitment (μM)
[R] (μM)
[S] (μM)
C)
[R]
Basal Recruited [S] (μM)
[R] = 5 μM
[R] = 0.5 μM
[S] (μM)
D)
Max Recruitment
Membrane Recruited [S]
Max Recruitment
Time
E)
Max Recruitment (μM)
[R] (μM)
[S] (μM)
F)
[R]
Max Recruited [S] (μM)
[R] = 5 μM
[R] = 0.5 μM
[S] (μM)
G)
Fold Enrichment
Membrane Recruited [S]
a = Basal recruitment
b = Max recruitment
(a+b)/a = Fold Enrichment
Time
H)
Fold Enrichment
[R] (μM)
[S] (μM)
I)
[R]
Fold Enrichment ([R*S]+[RS])/([RS])
[R] = 0.5 μM
[R] = 5 μM
[S] (μM)
J)
t1/2 dissociation
Membrane Recruited [S]
t1/2 dissociation
Time
K)
t1/2 dissociation (sec)
[R] (μM)
[S] (μM)
L)
[R]
t1/2 Dissociation (sec)
[R] = 5 μM
[R] = 0.5 μM
[S] (μM)

Figure 5

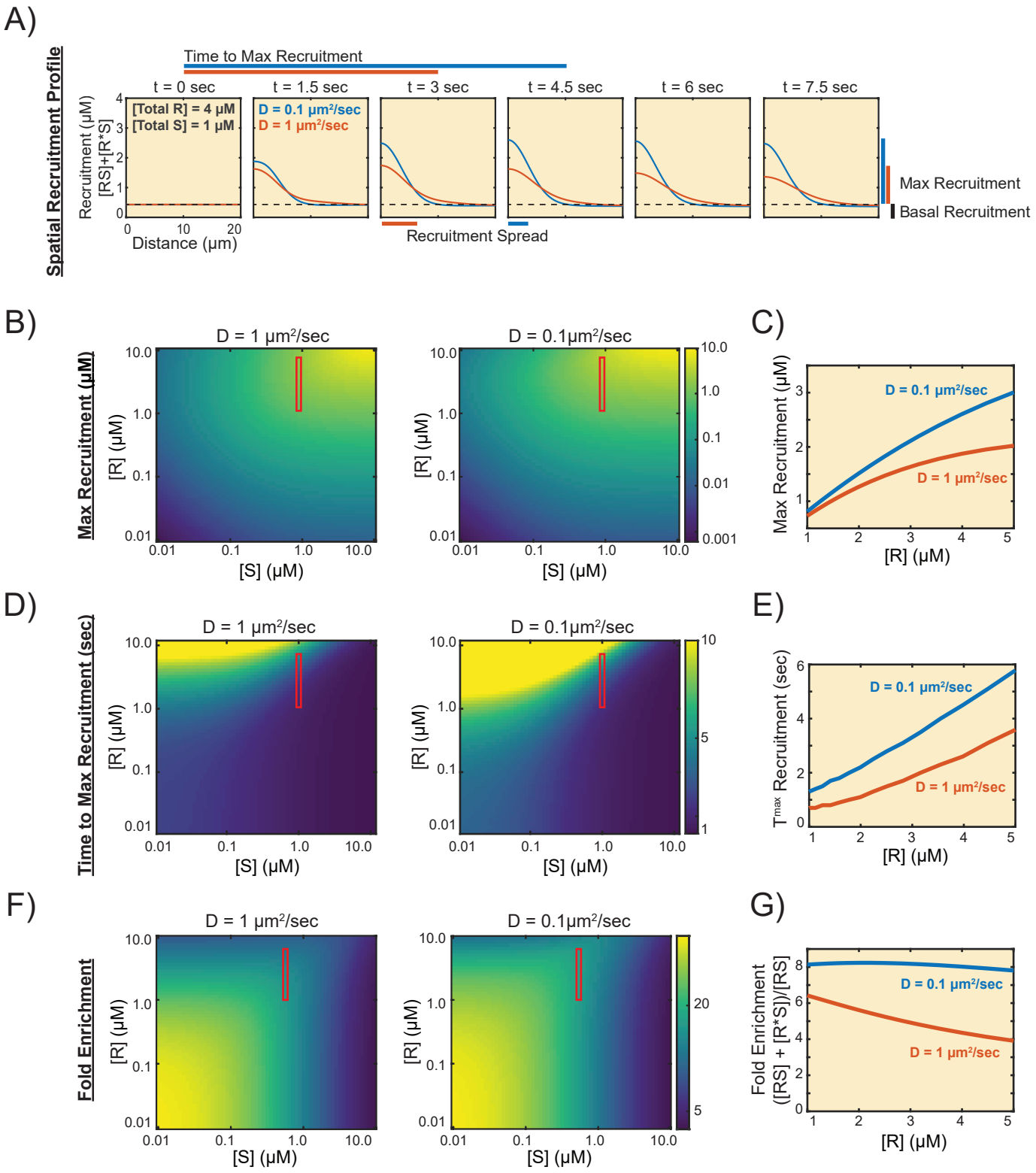
A)
Spatial Recruitment Profile
Time to Max Recruitment
t = 0 sec
t = 1.5 sec
t = 3 sec
t = 4.5 sec
t = 6 sec
t = 7.5 sec
[Total R] = 4 μM
[Total S] = 1 μM
D = 0.1 μm²/sec
D = 1 μm²/sec
Recruitment (μM) [RS]+[R*S]
Distance (μm)
Recruitment Spread
Max Recruitment
Basal Recruitment
B)
D = 1 μm²/sec
D = 0.1μm²/sec
Max Recruitment (μM)
[R] (μM)
[S] (μM)
C)
Max Recruitment (μM)
D = 0.1 μm²/sec
D = 1 μm²/sec
[R] (μM)
D)
Time to Max Recruitment (sec)
E)
Tmax Recruitment (sec)
F)
Fold Enrichment
G)
Fold Enrichment ([RS] + [R*S])/[RS]